Detonation Front Structure and the Competition for Radicals

Z. Liang, S. Browne, R. Deiterding, and J. E. Shepherd

California Institute of Technology, Pasadena, CA 91125 USA

Abstract

We examine the role of competition for radical species in determining detonation front structure for hydrogen and selected hydrocarbon fuels in air and oxygen. Numerical simulations and detailed reaction mechanisms are used to characterize the reaction zone length, shape, and sensitivity to temperature variation. We find that the effect of the competition for radicals on the energy release rate characteristics varies significantly for the chosen mixtures. Hydrogen exhibits a strong effect while in methane and ethane mixtures the effect is absent. Other hydrocarbons including acetylene, ethylene, and propane fall between these extreme cases. This competition is manifested by a peak in effective activation energy associated with a shift in the dominant reaction pathway in the initial portion of the reaction zone. The peak of the effective activation energy is centered on the extended second explosion limit. A five-step, four species reaction model of this competition process has been developed and calibrated against numerical simulations with detailed chemistry for hydrogen. The model includes a notional radical species and reactive intermediate in addition to reactants and products. The radical species undergoes chain-branching and there is a competing pathway through the reactive intermediate that is mediated by a three-body reaction followed by decomposition of the intermediate back to the radical species. We have used this model in two-dimensional unsteady simulations of detonation propagation to examine the qualitative differences in the cellular instability of detonation fronts corresponding to various degrees of competition between the chain-branching and reactive intermediate production. As the post-shock state approaches the region of competition between the radical and reactive intermediate, the detonation front becomes irregular and pockets of the reactive intermediate appear behind the front, but the detonation continues to propagate.

Keywords: detonation, chain-branching, extended limit, cell structure

1. Introduction

Simplified chemical reaction mechanisms have been widely used in multi-dimensional, unsteady simulations of detonations. In the last two decades, many different approaches have been taken to develop more realistic models that are still computationally efficient [1–3]. Simple ad hoc models [4–7] have also been

developed. These are in some sense an elaboration of the one-step model, using a notional reaction scheme with multiple steps between a set of pseudo-species in order to mimic the chemical processes that lead to complex two-dimensional detonation structure. It is with this type of simplified reaction modeling that the present paper is concerned.

Recent analyzes [8] of the role of chemical kinetics and the development of simplified models [4–7] for modeling detonation structure emphasize the role of radical species such as OH, which has now been directly visualized in experiments [9, 10]. A recurring theme in the development of simplified models is the competition for radical species associated with chain-branching and chain-termination steps with very different temperature and pressure dependence. This competition is particularly noticeable in detonations in hydrogen [11] and is associated with the idea of weak and strong ignition [12] and the extended second explosion limit [13]. The simplest representation of this effect is to characterize the extended second limit by a cross-over temperature where chain-branching and chain-termination reaction rates are equal. The naive view of the situation is that above this temperature branching dominates, while below, termination will quench the reaction. The situation with realistic combustion chemistry is more subtle and although chain-termination may alter the explosion time, peroxide chemistry may ultimately still enable an explosion to occur [13]. This is observed in both modeling studies [11, 14] and experiments [15–17] which show that detonations can be initiated at and below the extended second limit.

The characteristics of the reaction zone structure are observed to play a significant role in determining the unsteady front geometry. In particular, computation of unsteady one-dimensional detonations [5, 8, 21, 22] show that with increasing effective activation energy and decreasing energy release time (in comparison with the induction time), the leading shock amplitude oscillations become increasingly large and for sufficiently large value, the detonation propagation ceases. In two dimensions, using one-step models, it is found that with increasing effective activation energy [23, 24] and for marginal detonations [25, 26] the cellular structure becomes increasingly irregular and cellular substructure appears. Less extensive results are available for multi-dimensional simulations with detailed chemistry [27–30]. Inaba and Matsuo [27] studied the effects of channel width, initial pressure, and dilution on detonation cellular structure using a detailed chemical model. Their results showed transverse detonations as well as complex double Mach structures as the shock front oscillated and post-shock states traversed the cross-over region. Despite the extensive work on this subject, the issue of radical competition in multi-dimensional detonations and the possibility of the cross-over effect creating an intrinsic limit to propagation of cellular detonation fronts is not well understood.

The radical competition effect is incorporated into the three-step model [4, 5], which has been used to study various aspects of detonation initiation [18] and propagation [19]. One of the key conclusions of these studies [5, 18] with the three-step model is that the cross-over temperature provides a means of defining absolute limits (as first suggested by [20]) to the propagation and initiation of detonations. These proposals have motivated the present study and prompted us to examine the chemical bases for simplified models incorporating competition for radical species and more generally, the significance of the extended limit to detonation modeling.

2. Detailed Chemistry Results

Propagating detonations are unsteady and spatially nonuniform, but for the present purposes, it is necessary to adopt a greatly simplified model of the physical processes in order to examine the chemical aspects in some detail. We have used the constant-volume explosion model with initial conditions that are representative of the post-shock states in detonation waves. Our simulations [31] were done with Matlab using the Cantera package [32] to implement realistic thermochemistry and detailed chemical reaction mechanisms. We have used GRImech [33] for the hydrogen, methane, and ethane computations and the Wang et. al. mechanism [34, 35] for the acetylene, ethylene, and propane computations. All computations discussed are for stoichiometric fuel-air mixtures initially at 300 K and 1 atm unless otherwise stated.

In high-temperature, shock-induced combustion, the reaction zone consists of an induction period characterized by the induction time τ_i followed by an exothermic recombination period characterized by the energy release pulse width τ_e. The temperature sensitivity of the induction time is conventionally characterized by an effective activation energy, E_a [36, 37]. Stability computations, numerical simulations, and experimental studies of detonation structure [9] have shown that the reduced effective activation energy, $\theta = E_a/(\mathcal{R}T_s)$, where $\mathcal{R}$ is the ideal gas constant and T_s is the post-shock temperature, is a figure of merit for judging stability [6, 19]. Larger values of θ lead to more irregular cellular structure. More recently, theoretical studies [6] and numerical simulations [8] suggest that multiplying θ by a parameter proportional to τ_i/τ_e provides a better figure of merit for this purpose. These observations suggest that improvements in simplified reaction models will result from being able to independently adjust both θ and τ_i/τ_e, which is not possible with a one-step model. Contours of these parameters in the post-shock temperature-pressure plane are shown in Fig. 1 for hydrogen.

In hydrogen combustion, the ignition process begins with an initiation step which creates a small amount of radicals. Following the generation of the initial seed amounts of HO_2 and H, one of two pathways is followed. At high temperature and low pressure, the dominant initial process is chain-branching

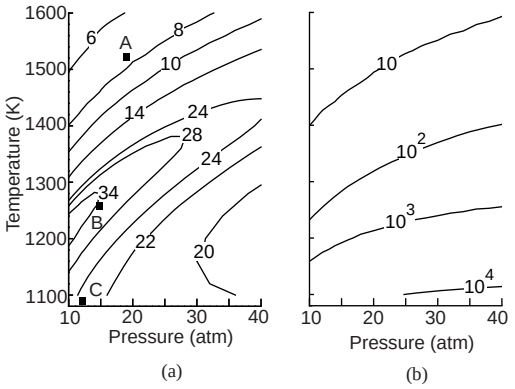

Fig. 1: Contours of (a) θ and (b) τ_i/τ_e for H_2. Post-shock states shown in (a) – A: $\phi = 1$ (29.6% H_2), B: $\phi = 0.5$ (17.4% H_2), C: $\phi = 0.35$ (12.8% H_2)

which results in exponential growth of H, O, and OH. At low temperature and high pressure, the dominant initial process creates HO_2 through the so-called "chain-termination" reaction. In vessel explosions at low temperatures (300-400°C), the HO_2 is sufficiently nonreactive, but in detonations [11], the temperature is still sufficiently high (> 900°C) that the HO_2 reacts, ultimately creating OH radicals which feed into the chain-branching pathway and enable the explosion. In either case, near the end of the branching-chain process the main energy release occurs through the recombination reaction of H and OH. The five-step model that we propose in Section 3 incorporates these features. The trade-off between pathways is a strong function of temperature and pressure; our five-step model includes two three-body reaction steps in order to capture this behavior.

In early discussions of the competition between chain branching and termination [13], the temperature-pressure plane was divided into two regions separated by a single curve obtained by equating the ratio of reaction rates for the chain-branching reaction and the chain-termination reaction to a specified value of order one. The cross-over temperature that is used in the three-step models is a pressure-independent parameter that mimics this effect. However, it is clear from the plot of $\theta(P,T)$, that the competition occurs over a wide range of $T(P)$. This is indicated by the broad "ridge" of high values of θ seen in Fig. 1a.

Similar exploration of the post-shock temperature-pressure plane for methane and ethane shows that the induction times and activation energies are monotonic and smoothly varying functions of pressure and temperature. Hence, for these mixtures, we conclude that there is no significant cross-over effect manifested in the coupling between chemistry and gas dynamics. Computations for ethylene and propane show a very modest increase in θ ($< 0.4\,\theta_{min}$) in the T-P region where a strong increase in θ ($> 6\,\theta_{min}$) is observed for H_2 mixtures. Computations for acetylene exhibit an intermediate increase in θ ($\approx 2\,\theta_{min}$). The notion of a cross-over temperature does not appear sufficiently well-defined and universal to form the basis of a theory of detonation limits.

Hydrogen exhibits the strongest cross-over effect, but rather than a single temperature, we find that there is a broad transition region characterized by substantial changes in θ and τ_i/τ_e. In contrast to the findings [5, 18] based on the three-step model, experimental results [11, 15] indicate that detonations in hydrogen and air can be successfully initiated and propagated at states (B and C on Fig. 1a) characterized as being within or below the cross-over region. The significant variations in θ and τ_i/τ_e will almost certainly be important for detonation structure even for mixtures with von Neumann points above this regime since substantial oscillations in the shock front velocity ($0.8U_{CJ}$ to $1.4U_{CJ}$) will result in some post-shock states within or below the cross-over regime.

3. Numerical Model

3.1. Five-Step Chemical Model

Based on the results of the chemical reaction kinetics simulations discussed above, we conclude a new type of simplified model is required to reproduce the reaction zone features that we observe in the H_2-O_2 system near the extended second limit. In particular, we would like to reproduce the two pathways for oxidation: the branching-chain for H atoms, and the straight-chain production of HO_2 and H_2O_2. The model should mimic the competition between these processes, the resulting induction time, energy release time, and effective activation energy dependence on temperature and pressure.

Our proposed scheme is,

$$R + M \xrightarrow{k_1} B + M \qquad \text{(S1)}$$

$$R + B \xrightarrow{k_2} B + B \qquad \text{(S2)}$$

$$R + B + M \xrightarrow{k_3} C + M \qquad \text{(S3)}$$

$$C + M \xrightarrow{k_4} B + B + M \qquad \text{(S4)}$$

$$B + B + M \xrightarrow{k_5} P + M \qquad \text{(S5)}$$

where R represents the pseudo-reactants (H_2 or O_2), B is the chain radical (H, O, or OH), C is the intermediate species (HO_2 or H_2O_2), P is the product (H_2O), and M is a chaperon molecule. S1 represents initiation producing the radical species B from the reactants R, S2 is chain-branching multiplication of B, S3 is the chain-termination competing with S2 for B, S4 is the dissociation of C back into B, and S5 is the final recombination reaction terminating in products P.

A modified Arrhenius rate constant formulation is

used for all steps.

$$r_1 = \rho Y_R \frac{A_1}{\bar{W}} \exp(-\frac{E_1}{\mathcal{R}T}) \quad (1)$$

$$r_2 = \rho Y_R Y_B \frac{A_2}{\bar{W}} \exp(-\frac{E_2}{\mathcal{R}T}) \quad (2)$$

$$r_3 = \rho \frac{\rho}{T} Y_R Y_B \frac{A_3}{\bar{W}W} \quad (3)$$

$$r_4 = \rho Y_C \frac{A_4}{\bar{W}} \exp(-\frac{E_4}{\mathcal{R}T}) \quad (4)$$

$$r_5 = \rho \frac{\rho}{T} {Y_B}^2 \frac{A_5}{\bar{W}W} \quad (5)$$

where A and E are the pre-exponential constant and activation energy respectively, which maintain constant values, and ρ and T are the density and temperature which evolve with the simulation. $\bar{W}$ is the average molecular weight given that the molecular weights for R, B, C and P are W, W, $2W$, and $2W$ respectively. To mimic dilution, we include an inert species, N, with a molecular weight of $2W$. We assume that the energy release is only associated with S5, i.e. only the heat of formation of the product, $h^0_{f,P}$, is nonzero, and we use the perfect gas equation of state.

The rate constant values were chosen by analogy to those in the H_2-O_2 mechanism with some adjustment by trial and error using constant-volume explosion computations and comparing the parameters θ and τ_i/τ_e with results from the detailed reaction mechanism. A set of parameters developed for modeling stoichiometric H_2-O_2 with 85% argon dilution is summarized in Table 1. Figure 2 compares values

Table 1: Five-Step Model Parameters.

W	0.017	kg/mol
$\bar{W}$	0.033	kg/mol
$E_1/\mathcal{R}$	24131	K
$E_2/\mathcal{R}$	8383	K
$E_4/\mathcal{R}$	22980	K
γ	1.5	
$h^0_{f,P}/\mathcal{R}T_0$	-3030.3	mol/kg
Y_N	0.919	
A_1	1.37×10^9	m^3/kg/s
A_2	1.32×10^8	m^3/kg/s
A_3	7.0×10^5	m^3/kg/s
A_4	3.23×10^9	m^3/kg/s
A_5	1.37×10^9	m^3/kg/s

of θ and τ_i/τ_e from constant volume simulations with both the detailed chemistry model and the five-step model. In our model development, we focused on duplicating the low temperature and pressure behavior. For this reason, at higher temperatures and pressures, there are larger differences between the 5-step model and detailed chemistry but the values have the correct order of magnitude and trends.

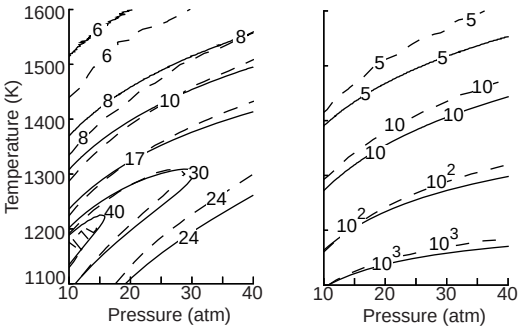

Fig. 2: Contours of (a) θ and (b) τ_i/τ_e for the five-step model (solid) and detailed chemistry (dashed) for stoichiometric H_2-O_2 with 85% argon dilution

3.2. Numerical Method

The unsteady propagation of a detonation front is modeled using the two-dimensional (planar), inviscid, nonconducting, reactive Euler equations with the perfect gas equation of state and the five-step model. The equations are solved with an explicit second order Godunov-type numerical scheme incorporating a hybrid Roe-solver-based method. A time-operator splitting technique is employed to decouple hydrodynamic transport and chemical reaction. A block-structured adaptive mesh refinement technique is utilized to supply the required resolution locally on the basis of hydrodynamic refinement criteria [30]. This adaptive method uses a hierarchy of spatially refined subgrids which are integrated recursively with reduced time steps.

A rectangular two-dimensional computational domain was considered. Upper and lower boundaries were no-slip solid walls, and zero gradient inflow and outflow were imposed on the right and left boundaries. The unreacted mixture enters the computational domain from the right with specified initial parameters T_o, P_o, and U_{CJ}. A planar ZND profile was initially placed approximately 10 induction lengths away from the right boundary, and an unreacted hot pocket was placed to the left of the shock in the burned products for Cases 1 and 2 (Section 4) and to the right of the shock in the unburned reactants for Case 3. A domain height of 30 induction lengths and a width of 50 induction lengths were chosen for our computations giving an effective resolution of 64 points per induction length.

4. Simulation Results and Discussion

We have carried out parametric computations to explore consequences of our model. As discussed above, conditions in each regime of the θ plane (above, below, and within the competition region) are of interest. The three cases discussed below are not

Table 2: Physical parameters for three computation cases with P_o =1 atm and T_o =295 K.

Case	Y_N	$\bar{W}$ (g/mol)	U_{CJ} (m/s)	U/U_{CJ}	P_s (atm)	T_s (K)	Δ_i (mm)	θ	τ_i/τ_e
1	0.857	29.8	1785	1.0	30.7	2094	0.029	4.3	0.9
				0.85	22.1	1587	0.16	7.2	1.5
2	0.901	30.9	1481	1.0	21.9	1575	0.24	7.3	1.2
				0.85	15.8	1210	14.6	16.	5.6
3	0.913	31.3	1390	1.0	19.5	1432	0.64	10	1.3
				0.85	14.0	1108	275	29	33

intended to simulate specific chemical mixtures; instead they are chosen to qualitatively demonstrate the behavior of our model as post-shock conditions approach the competition region.

Physical parameters for the three cases we studied are given in Table 2, and all other parameter values are given in Table 1. The von Neumann states (T_N,P_N) for all cases remain above the competition region, but shock front oscillations of $U < U_{CJ}$ give post-shock states close to the competition region. The induction zone length Δ_i is a strong function of the post-shock temperature and for this reason varies by a factor of 20 between Case 1 and Case 3 at U_{CJ}. As the shock oscillates from U_{CJ} to $0.85U_{CJ}$, θ, τ_i/τ_e, and Δ_i increase from their CJ values. For each case, θ increases by factors of 0.6, 1.2, and 1.8 and τ_i/τ_e with factors of 0.4, 3.6, and 25 respectively. Again, due to its temperature sensitivity, Δ_i increases most dramatically with factors of 4.6, 60, and 430 respectively. We expect that detonation stability will decrease as these three parameter values increase. The appearance of the front and following flow (Figs. 3a, 5a, & 6a) for these three cases qualitatively agrees with this trend.

Fig. 3 shows results for temperature and mass fraction fields for Case 1 after the initial transient has settled down. A single, regular detonation cell fills the channel and a keystone-like feature is clearly visible in the mass fraction fields. A two triple-point structure is created at the juncture of the transverse wave and main shock front. The transverse wave strength ($\Delta P/P$) for the portion between the first and second triple point is 0.75, while it is 2.0 beyond the second triple point. The stronger transverse wave propagates along the induction zone and burns the material behind the incident wave with the exception of a thin layer in the vicinity of the primary triple point. Similar structures have been observed in numerical simulations with detailed chemistry for H_2-O_2-Ar mixtures by Hu et. al [38] and with the four-step model of Liang and Bauwens [7]. The overall appearance of the numerical simulation is also similar to the experimental images for H_2-O_2-Ar mixtures presented in Pintgen et. al [10].

The cellular structures of Cases 2 and 3 are much more irregular than Case 1. For these irregular cases, at early times (not shown in this paper) the structure appears identical. The transverse waves are strong and fine cellular structures develop and propagate into the long induction zone exhibiting similar characteristics to the transverse detonations structures observed by Gamezo et. al in marginal detonations [26]. Also sub-detonation structures develop behind the strong part of the leading shock which agrees well with Gamezo et. al's observations that when θ is greater than 6.5, secondary detonation cells will appear.

At later times, the cellular structure of Cases 2 and 3 begins to deviate. For Case 2, as shown in Figs. 4 and 5, the major triple point remains obvious, but transverse waves weaken and cease to react. In the first two frames of Fig. 4, as the Mach wave moves up toward the top of the channel, sub-cellular structures couple with the leading shock front and unburnt pockets form a "tunnel" or "funnel." After the Mach wave collides with the wall and moves back toward the bottom of the channel, cellular sub-structures begin decoupling from the front and the induction zone behind the incident wave lengthens. Partially reacted pockets convect away from the detonation front. In the mass fraction fields shown in Fig. 5, small keystones shapes can be seen on the leading front. These are apparently burned after the sub-structure decouples from the front.

For Case 3, as shown in Fig. 6, the front becomes much more complex and numerous transverse waves are present. Islands of partially-reacted gas become isolated downstream of the main detonation front and appear similar to the experimental observations for nitrogen-diluted mixtures in Pintgen et. al [10]. Experimental soot foils [10] indicate a wider range of cell sizes, and in their Schlieren images, the leading shock wave appears to be much less planar than for the argon-diluted mixture with the same cell size.

5. Summary

We have examined the competition for radical species and how it is manifested in the steady and unsteady structure of detonation fronts. The classical example of competition for H radicals occurs in the hydrogen-oxygen system, and this has previously been characterized in terms of the extended second limit. We have examined this phenomena and looked for similar effects in hydrocarbons through a series of numerical simulations using detailed chemical reac-

tion mechanisms for hydrogen and selected hydrocarbon fuels. Examining the variation of induction time, energy release time, and effective activation energy for these mixtures shows that the competition for radicals has varying effects for different fuels.

In mixtures with hydrogen as fuel, the competition for H atoms produces a broad zone of high effective activation energy in the temperature-pressure plane. The peak of the activation energy appears coincident with the classical extended second limit as specified by reaction rate ratios, but previous experiments show that detonations can be initiated and propagated with von Neumann states below the cross-over region. There are significant implications for initiation and propagation due to the large values θ and τ_i/τ_e near the cross-over region in hydrogen, but this apparently does not preclude the existence of detonations in this regime.

In mixtures with hydrocarbon fuels, the effects of competitions for radicals vary. In methane and ethane mixtures, the effects are absent, and in ethylene and propane mixtures the effects are modest. Acetylene is the only hydrocarbon studied that exhibits behavior similar to hydrogen, although the effects are considerably less than that seen in hydrogen mixtures. Our interpretation is that such competitive effects certainly exist in these mechanisms but there are many routes for H-atom production and consumption. As a consequence, the concept of the cross-over temperature does not appear to be universal.

Examination of the results of simulations with detailed reaction mechanisms indicates that a realistic simplified model must include the subsequent reactions of the products of the termination reaction that compete with chain branching. A simplified reaction mechanism that is useful for unsteady detonation simulations must match the dependence of Δ_i, θ, τ_i/τ_e on temperature and pressure over the range shown to be relevant to unstable waves. We have presented a five-step model that achieves this for hydrogen by incorporating two competing reaction pathways that represent the chemical processes that are observed in the detailed simulations.

We have explored the consequences of our model as the post-shock state approaches the competition region in the temperature-pressure plane. While the three cases presented do not represent specific chemical mixtures, we have qualitatively compared two-dimensional detonation simulation results using our model with experimental results. Von Neumann states far from the competition region exhibit regular cellular structure similar to experimental results with significant argon dilution. On the other hand, states closer to the competition region exhibit irregular structures like those observed experimentally for nitrogen-diluted H_2-O_2 systems. In these irregular structures, we see pockets of low-temperature intermediates which support the inclusion in our model of reactions mimicking peroxide chemistry. Previous studies with one-step models and high activation energy have also shown these pockets but have interpreted these as non-reactive since no other pathways for low-temperature reaction are possible. Our results show that these pockets are actually partially reacted material and that after a sufficient time, the reaction pathway corresponding to the peroxide chemistry will result in explosion of these regions.

Finally, it should be clear that our simulations with both detailed chemistry and the simplified model have significant limitations. In the case of the detailed chemistry we have only examined the steady-state structure of the reaction zone and we have not attempted to deal with the significant issue of unsteadiness [39]. Our unsteady simulations have only examined situations above the competition region and we have not attempted to examine the region within and below the "ridgeline" of high activation energy seen in Fig. 1. The very large values of τ_i/τ_e for mixtures in this region also pose a significant challenge for numerical simulation. The extension of our simple five-step model to hydrocarbon mixtures and the application to simulating highly unstable fronts observed in hydrocarbon-air mixtures also remains to be studied.

Acknowledgments

Z. Liang is supported by a Fellowship from NSERC, Canada and S. Browne is supported by an NSF Graduate Fellowship. We thank D. Meiron of DOE ASC Alliance Center for the Simulation of Dynamic Response of Materials at the California Institute of Technology for computing facilities and supporting AMROC development. D. Goodwin of the California Institute of Technology provided substantial assistance with using Cantera. H. Wang of the University of Southern California provided advice on using his C3 reaction mechanism and extending the thermodynamic data to detonation conditions.

References

[1] C. A. Eckett, *Numerical and Analytical Studies of the Dynamics of Gaseous Detonations*, Ph.D. thesis, California Institute of Technology, Pasadena, California (September 2000).

[2] B. Varatharajan, F. A. Williams, *J. Propulsion Power* 18 (2) (2002) 344–351.

[3] T. F. Lu, C. K. Law, Y. G. Ju, *Journal of Propulsion and Power* 19 (5) (2003) 901–907.

[4] J. W. Dold, A. K. Kapila, *Combust. Flame* 85 (1991) 185–194.

[5] M. Short, J. J. Quirk, *J. Fluid Mech.* 339 (1997) 89–119.

[6] M. Short, G. J. Sharpe, *Combust. Theor. Model.* 7 (2) (2003) 401–416.

[7] Z. Liang, L. Bauwens, *CTM* 9 (2005) 93–112.

[8] M. I. Radulescu, H. D. Ng, J. H. S. Lee, B. Varatharajan, in: *Proc. Combust. Inst.*, Vol. 29, 2002, pp. 2825–2831.

[9] J. M. Austin, F. Pintgen, J. E. Shepherd, in: *Proc. Combust. Inst.*, Vol. 30, 2005, pp. 1849–1857.

[10] F. Pintgen, C. A. Eckett, J. M. Austin, J. E. Shepherd, *Combust. Flame* 133 (2003) 211–229.

[11] J. E. Shepherd, *Prog. Astronaut. Aeronaut.* 106 (1986) 263–293.

[12] J. W. Meyer, A. K. Oppenheim, in: *13th Symp. (Intl) on Combustion*, 1970, pp. 1153–1164.
[13] V. V. Voevodesky, R. I. Soloukhin, in: *10th Symp. (Intl) on Combustion*, 1965, pp. 279–283.
[14] J. E. Dove, T. D. Tribbeck, *Astronautica Acta* 15 (1970) 387–397.
[15] S. R. Tieszen, M. P. Sherman, W. B. Benedick, J. E. Shepherd, R. Knystautas, J. H. S. Lee, in: *Prog. Astronaut. Aeronaut.*, Vol. 106, 1986, pp. 205–219.
[16] D. W. Stamps, S. R. Tieszen, *Combust. Flame* 83 (3-4) (1991) 353–364.
[17] D. W. Stamps, S. E. Slezak, S. R. Tieszen, *Combust. Flame* 144 (1-2) (2006) 289–298.
[18] H. D. Ng, J. H. S. Lee, *J. Fluid Mech.* 476 (2003) 179–211.
[19] M. Short, A. K. Kapila, J. J. Quirk, *Phil. Trans. R. Soc. Lond.* A 357 (1999) 3621–3637.
[20] F. E. Belles, in: *7th Symp. (Intl) on Combustion*, 1959, pp. 745–751.
[21] L. He, J. Lee, *Phys. Fluids* 7 (1995) 1151–1158.
[22] H. D. Ng, A. J. Higgins, C. B. Kiyanda, M. I. Radulescu, J. H. S. Lee, *Nonlinear dynamics and chaos analysis of one-dimensional pulsating detonations* (2005).
[23] A. M. Khokhlov, J. M. Austin, F. Pintgen, J. E. Shepherd, *Numerical study of the detonation wave structure in ethylene-oxygen mixtures*, 42nd AIAA Aerospace Sciences Meeting and Exhibit, January 5-8, 2004, Reno, NV, AIAA 2004-0792 (2004).
[24] D. D. V. N. Gamezo, E. S. Oran, *Combust. Flame* 116 (1999) 154–165.
[25] M. I. Radulescu, G. J. Sharpe, J. H. S. Lee, C. B. Kiyanda, A. J. Higgins, R. K. Hanson, in: *Proc. Combust. Inst.*, Vol. 30, 2005, pp. 1859–1867.
[26] V. N. Gamezo, A. A. Vasilev, A. M. Khokhlov, E. Oran, in: *Proc. Combust. Inst.*, Vol. 28, 2000, pp. 611–617.
[27] K. Inaba, A. Matsuo, *Cellular Structures of Planar Detonations with a Detailed Chemical Reaction Model*, 39th AIAA Aerospace Sciences Meeting and Exhibit, January 8-11, 2001, Reno, NV, AIAA 2001-0480 (2001).
[28] E. S. Oran, J. W. Weber, Jr., E. I. Stefaniw, M. H. Lefebvre, J. D. Anderson, Jr., *Combust. Flame* 113 (1998) 147–163.
[29] X. Y. Hu, D. L. Zhang, B. C. Khoo, Z. L. Jiang, *Shock Waves*DOI: 10.1007/s00193-004-0234-5.
[30] R. Deiterding, *Proc. Tenth International Conference on Hyperbolic Problems: Theory, Numerics, Applications*.
[31] S. Browne, J. E. Shepherd, *Numerical Solution Methods for Control Volume Explosions and ZND Detonation Structure* (2005).
[32] D. Goodwin, *Cantera: Object-Oriented Software for Reacting Flows*, Tech. rep., California Institute of Technology, http://www.cantera.org (2005).
[33] G. Smith, D. Golden, M. Frenklach, N. Moriarty, B. Eiteneer, M. Goldenberg, C. Bowman, R. Hanson, S. Song, W. G. Jr., V. Lissianski, Z. Qin, *GRI-MECH 3.0*, http://www.me.berkeley.edu/gri_mech/.
[34] H. Wang, A. Laskin, *A Comprehensive Kinetic Model of Ethylene and Acetylene Oxidation at High Temperatures*, Tech. rep., Department of Mechanical Engineering, University of Deleware (1998).
[35] Z. Qin, V. Lissianski, H. Yang, W. Gardiner, S. Davis, H. Wang, in: *Proc. Combust. Inst.*, Vol. 28, 2000, pp. 1663–1669.
[36] E. Schultz, J. Shepherd., *Validation of detailed reaction mechanisms for detonation simulation.*, Tech. Rep. FM99-5, GALCIT (2000).
[37] F. Pintgen, J. E. Shepherd, *Pulse Detonation Engine Impulse Analysis for Partially-Oxidized Jet Fuel*, GALCIT Report FM2003.001 (2003).
[38] X. Y. Hu, D. L. Zhang, B. C. Khoo, Z. L. Jiang, *Combust. Theor. Model.* 8 (2004) 339–359.
[39] C. A. Eckett, J. J. Quirk, , J. E. Shepherd, *J. Fluid Mech.* 421 (2000) 147–183.

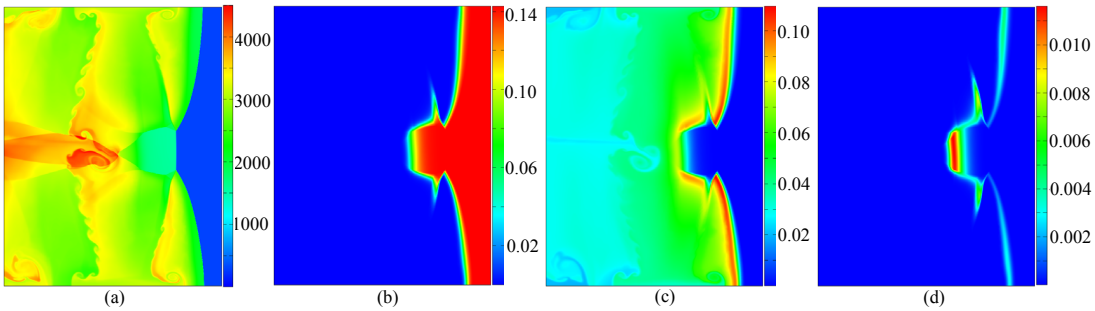

Fig. 3: Contours of (a) T, (b) Y_R, (c) Y_B, and (d) Y_C for Case 1.

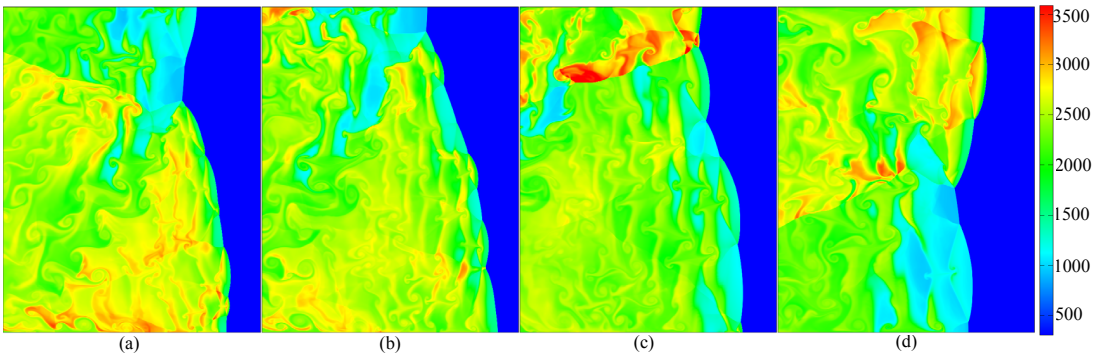

Fig. 4: Time sequence of contours of temperature field for Case 2.

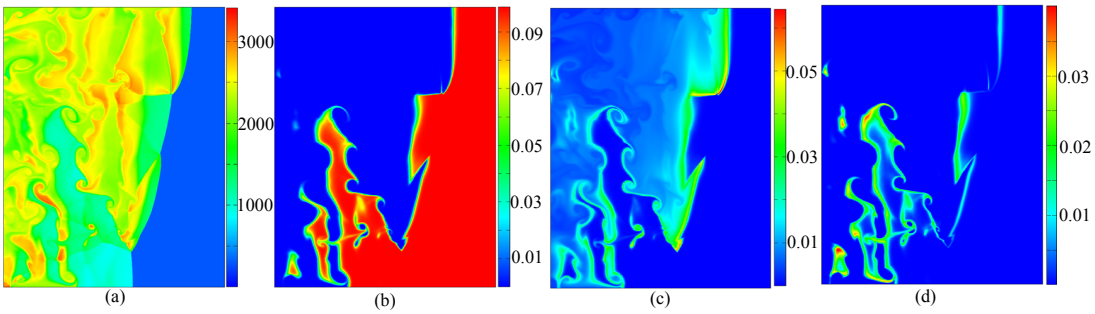

Fig. 5: Contours of (a) T, (b) Y_R, (c) Y_B, and (d) Y_C for Case 2.

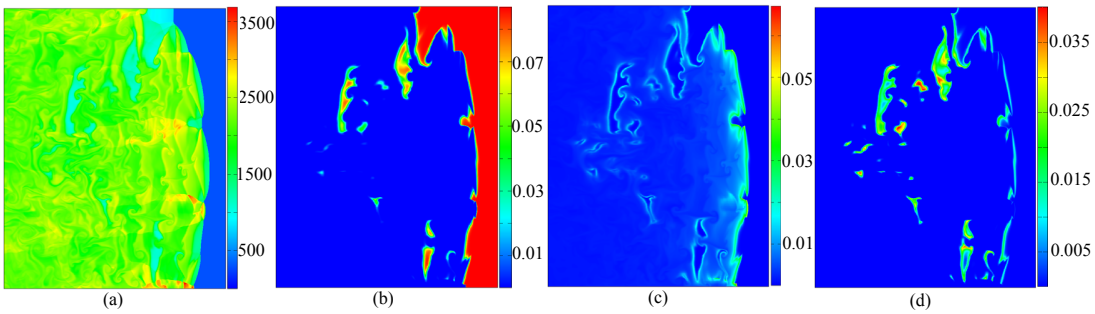

Fig. 6: Contours of (a) T, (b) Y_R, (c) Y_B, and (d) Y_C for Case 3.